

## DETERMINATION OF HOT PLASMA CHARACTERISTICS FROM *TRACE* IMAGES.

S. Gburek<sup>1</sup> and T. Mrozek<sup>2</sup>

<sup>1</sup>Space Research Centre, Polish Academy of Sciences, Solar Physics Division, 51-622 Wrocław, ul. Kopernika 11, Poland

<sup>2</sup>Astronomical Institute, Wrocław University, ul. Kopernika 11, 51-622 Wrocław, Poland

### ABSTRACT

Updated image formation model and accurate PSF function of the *TRACE* telescope are used for determination of flaring plasma parameters directly from individual *TRACE* EUV images. A new method for derivation of the temperature and emission measure of intense (flaring) kernels from a *single TRACE* image is presented and discussed in this respect. The method is based on interpretation of *TRACE* PSF diffraction pattern and the quantitative analysis of EUV kernels seen in higher orders. Calculated values of *TRACE*-derived temperatures are compared to those determined in X-rays using GOES data obtained simultaneously. The results yet obtained clearly indicate that a hot plasma ( $T > 5$  MK) can be diagnosed directly from *TRACE* images, in particular during the impulsive flare phase.

Key words: *TRACE*; solar flares.

### 1. INTRODUCTION

The Transition Region and Coronal Explorer (*TRACE*) satellite was launched on 2 April 1998 to perform observations of the Sun with high temporal and spatial resolution. The *TRACE* 30 cm Cassegrain telescope focuses the solar radiation on CCD sensor of the size of  $1024 \times 1024$  pixels (1 pixel = 0.5 arcsec). The telescope field of view is  $8.5 \times 8.5$  arcmin and spatial resolution is of  $\sim 1$  arcsec. A detail characteristic of the instrument can be found in Handy et al. (1999). A review of *TRACE* early observations is given by Schrijver et al. (1999).

*TRACE* is capable of taking solar images of solar atmosphere at wavelengths ranging from white light to EUV in a several preselected passbands. The *TRACE* EUV wavelength passbands are centered near 284 Å, 195 Å and 171 Å. Two of them

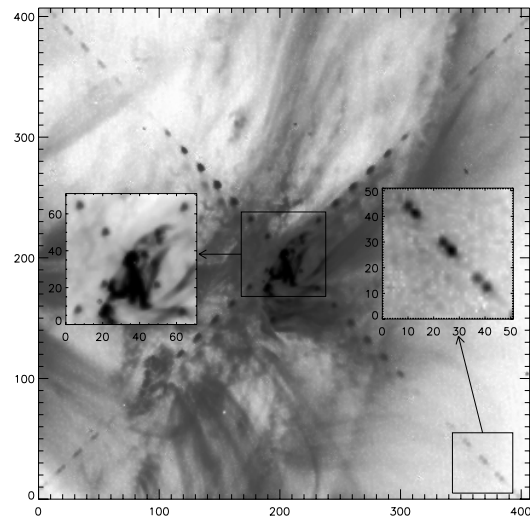


Figure 1. *TRACE* compact flare image with strong diffraction pattern.

the 171 Å and 195 Å passbands have been most frequently used for imaging solar flares what makes them particularly important for studying more energetic solar plasma phenomena. A characteristic feature which distinguishes the *TRACE* EUV images from those taken in other telescope passbands, is the presence of diffraction effects. The diffraction comes from fine nickel wire mesh which supports the entrance filters and acts as dispersion element for all the three EUV telescope channels. The diffraction effects are particularly well pronounced in images of strong compact sources as the one seen in Figure 1. From the inspection of *TRACE* intense flare images it follows that diffraction causes many subordinate structures of different intensities and shape to appear in data. These structures, are spaced roughly every 20 pixels and arranged along two lines intersecting at an almost right angle.

Due to diffraction about 20 % of the signal is spread

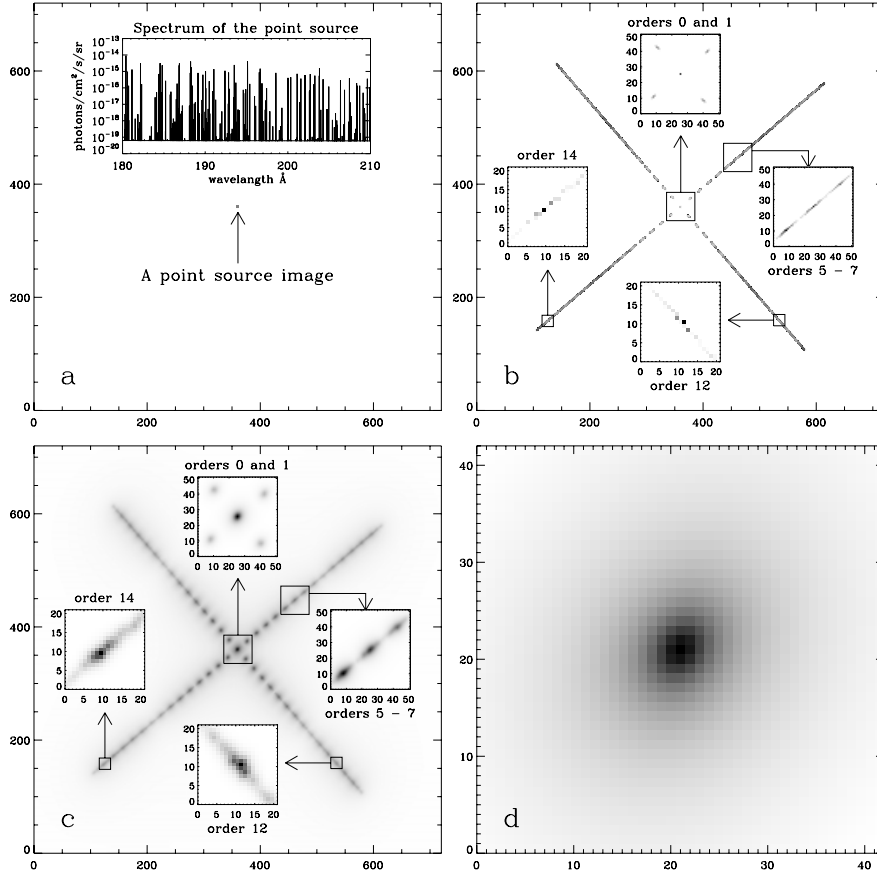


Figure 2. An image of a non-monochromatic point source as it would be seen on TRACE CCD is shown in the panel a). In the insert a spectrum of this source is plotted. In this example the solar isothermal spectrum ( $T = 1\text{MK}$ ) was chosen for simulations. Panel b) shows the image of the point source from a) convolved with diffraction portion of the TRACE PSF -  $P_{diff}$ . Panel c) shows the ultimate image of the source in a). This image arises as convolution of the diffraction pattern from b) with the TRACE PSF core part -  $P_{core}$  which is shown enlarged in d).

over the CCD far away from the main emission site. Hence, any good image formation model for TRACE EUV channels must account for diffraction effects.

In the next section we discuss the image formation model for TRACE EUV passbands with diffraction effects discussed in terms of TRACE point spread function (PSF). Possible applications of the above mentioned model to spectroscopic analysis of the TRACE data are shown further.

## 2. TRACE EUV IMAGE FORMATION MODEL

The accuracy of the TRACE telescope EUV images is limited mainly due to instrumental blur and noise contribution which comes from photon statis-

tics, CCD readout, digitization of the signal etc. The TRACE blurring pattern can be discussed in terms of the telescope point spread function (PSF) which describes the response of the entire optics to a distant point source. Assuming linear image formation model we can describe the relationship between the true observed brightness distribution  $I$  and its TRACE image  $D$  degraded by blur and noise using the following equation

$$D = I \otimes P + N \quad (1)$$

where  $P$  is the TRACE PSF,  $\otimes$  stands for a convolution operator and  $N$  is the noise contribution.

TRACE PSF function can be defined as two component function. First component  $P_{diff}$  defines only diffraction pattern caused by the entrance filter mesh. The second component  $P_{core}$  is the

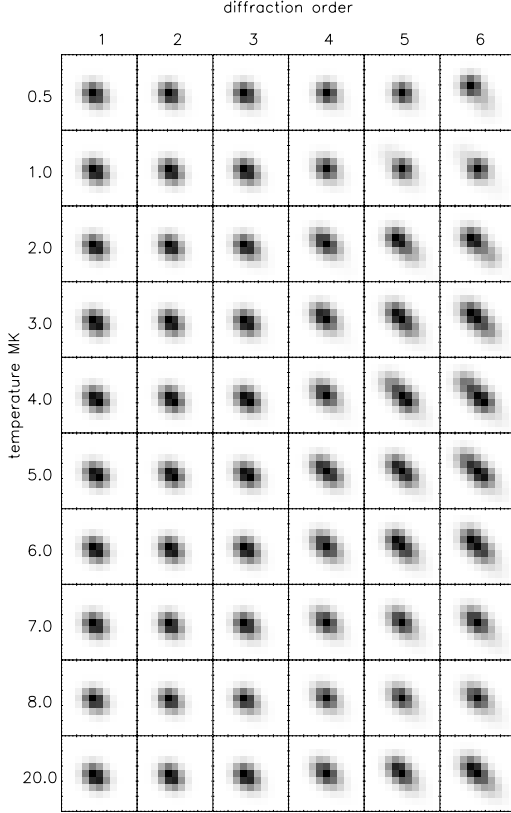


Figure 3. Calculated temperature-dependent shape of the TRACE PSF diffraction structures for low diffraction orders (Point-like source, lower-right diffraction pattern arm).

TRACE PSF core which describes the blur component that comes from other factors such as geometric imperfectness of telescope mirrors. Thus the expression for the entire TRACE PSF can be given as

$$P = P_{diff} \otimes P_{core} \quad (2)$$

The TRACE core PSF components for 171 Å and 195 Å passbands were determined using blind deconvolution approach (Gburek S. (2004)). They are of the form of single slightly elliptically deformed peak of full width at half maximum between 2.0 and 2.5 CCD pixel.

It has been checked in Lin, et al. (2001) that the TRACE diffraction PSF portion  $P_{diff}$  can be modeled theoretically using Fraunhofer diffraction theory. The theoretical model of TRACE  $P_{diff}$  also consists of cross-like arranged, separated structures. For a monochromatic point source these structures as seen on the CCD have a form of a delta function (the diffraction broadening of each peak is negligibly small in comparison to CCD pixel size) and arise

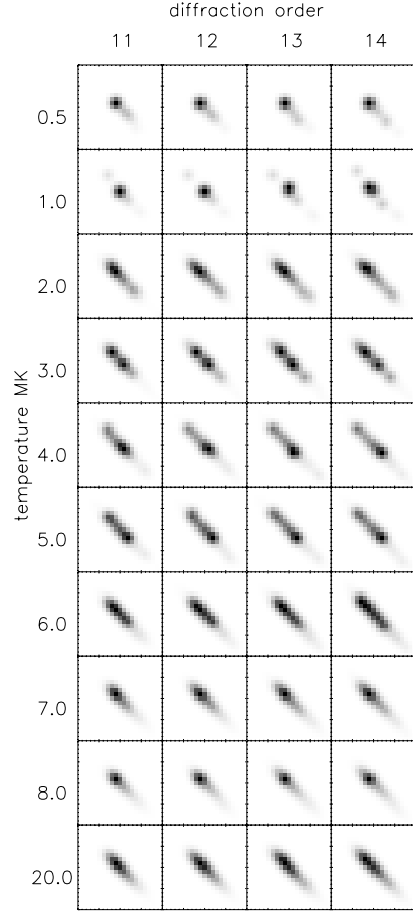


Figure 4. Calculated temperature-dependent shape of the TRACE PSF diffraction structures for higher orders (Point-like source, lower-right diffraction pattern arm).

as principal maxima of the diffraction pattern produced by 2D grating with square openings (Lin, et al. (2001)).

For non-monochromatic point sources only the zeroth order maximum (central 'white in EUV' peak of  $P_{diff}$ ) occupies a single pixel area. Due to dispersion effects, in higher orders one gets elongated structures which eventually separate further away from the  $P_{diff}$  center. This is clearly seen in Figure 2 where an example of the TRACE PSF generated for non-monochromatic point source is shown.

The theoretical model gives quantitative characteristic of all the observed diffraction effects. During the tests it appeared that PSF model shape strongly depends on temperature particularly in far diffraction orders. (see figures 3 and 4). This temperature variability of the PSF model gives therefore a possibility for temperature diagnostics in TRACE data. In the

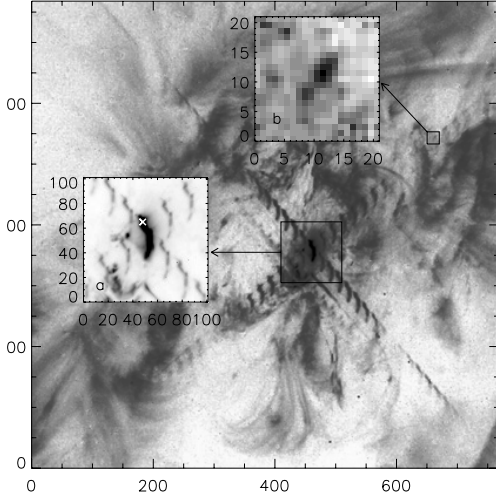


Figure 5. X1.0 flare image taken on 2002 August 21 at 05:31:45. Zoomed in a) is the central structure with the position of the brightest kernel marked by the white cross. This kernel was selected for fitting and determination of T&EM distribution. Zoomed in the box b) is the diffraction structure in twelfth order chosen for comparison between data and fit.

next section we show an example of such T&EM diagnostic for a *TRACE* image taken in 195 Å filter.

### 3. APPLICATIONS OF THE *TRACE* PSF TO DATA ANALYSIS

We selected for analysis the brightest kernel seen in X1.0 flare image (figure 5) taken on 2002 August 21. The central portion of this image is heavily saturated but a pronounced diffraction pattern is seen extending almost to the image edges. The actual position of the kernel emission site was determined from the positions of this kernel seen in first and second diffraction order. Next the signal near emission site was changed iteratively, blurred with the PSF models generated for different temperatures and compared to data. The comparison between fitted model and data took place in the twelfth diffraction order in the upper-right arm of diffraction pattern. We selected this image area for comparison because the structures seen there are superimposed on a relatively flat background, not corrupted by any defects and still have good signal to noise ratio.

Eventually we obtained a good quality fit (figure 6) with normalized ( $\chi^2 = 1.6$ ). From the fit we were capable of determining how much signal we get from the plasma at different temperatures. Then using *TRACE* temperature response curve for

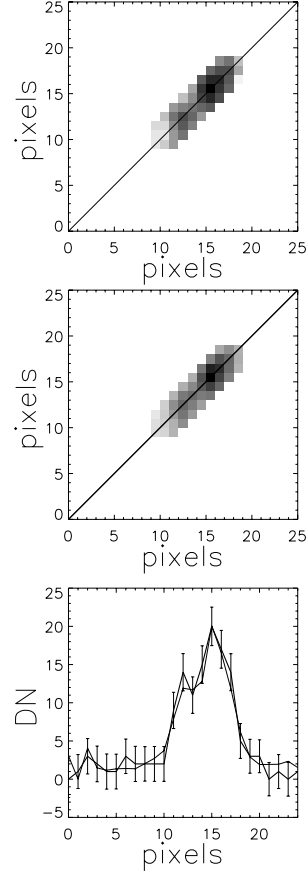


Figure 6. Top - the diffraction structure in twelfth order in the upper-right diffraction arm of the diffraction pattern shown in figure 5. Middle - calculated diffraction image (the same order and arm of the pattern) obtained from results of multi-temperature fit of the signal to data from the top panel. Bottom - a cut plot along the main diagonal of the data (thick solid line) and fit (thin solid line).

*TRACE* 195 Å channel (see figure 7) we converted the signal at each temperature to emission measure.

Thus we obtained the T&EM distribution for the investigated flare kernel which is shown in figure 8. A presence of a hot and a colder plasma component ( $T > 10$  MK) in the analyzed kernel can be identified from this plot.

These two components form a separated peak-shaped areas in twelfth order diffraction data used for fitting (see figure 9). Separation occur because for low temperatures emission at longer wavelength dominate the contribution to the *TRACE* observed signal in 195 Å passband. For high temperatures contribution of the emission at shorter wavelengths takes over. As it can be seen in 7) contribution from line

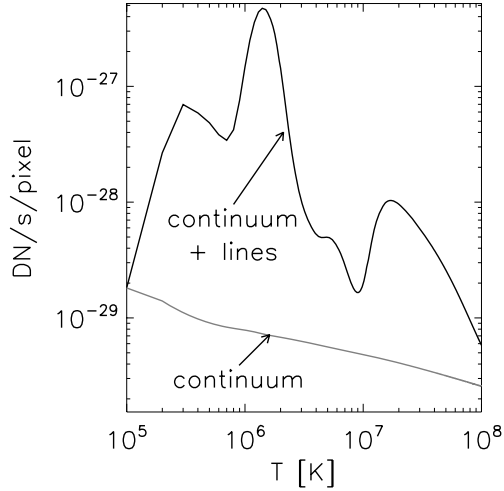


Figure 7. TRACE response curves for 195 Å passband for unite column emission measure.

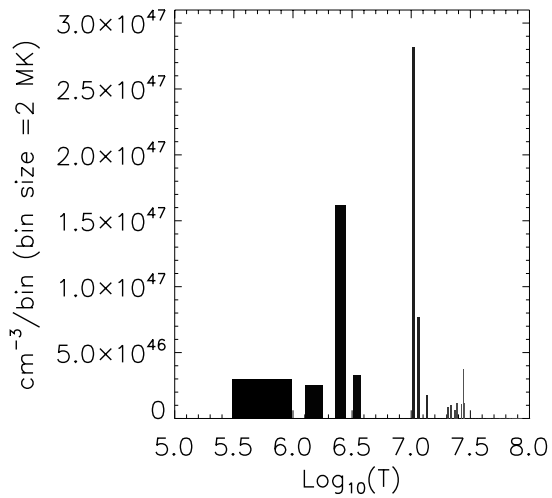


Figure 8.  $DEM(T)$  - determined from the multi-temperature fit to data.

emission is the main shaping factor for temperature response curve for *TRACE* 195 Å channel over the entire temperature range [0.1 - 100.0] MK. Of particular importance are the principal lines (an extensive study of the temperature response for *TRACE* 195 Å channel and contribution to the emission from continuum and lines was recently shown by Phillips et al. (2005)) which dominate the emission at certain temperature regimes. Six of these lines are listed

Table 1. Principal coronal lines contributing to the *TRACE* signal in 195 Å passband.  $T_{max}$  stands for the temperature in which line emission takes its maximum value.

No	Wavelength Å	Ion	$T_{max}$ [MK]
1	192.02	Fe xxiv	16.5
2	192.82	Ca xvii	5.4
3	193.87	Ca xiv	3.2
4	194.02	Ni xvi	2.5
5	195.12	Fe xii	1.4
6	196.54	Fe xiii	1.6

in table 1 and their emission curves are plotted in figure 10.

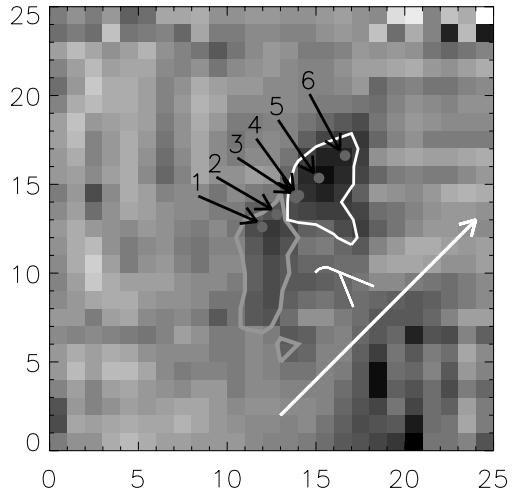


Figure 9. Data from twelfth diffraction order in the upper-right diffraction pattern arm. Principal coronal line positions (pointed by arrows) for *TRACE* in 195 Å passband are superimposed on the data. Line numbers are the same as in table 1. Contours are at the 0.8 level of the maximum intensity of contoured structure. The hot plasma component in the data is contoured in gray, the cold one is inside the white contour.

Positions of these lines are also superimposed on twelfth order diffraction data in figure 9. It is seen there that position of the confined structure located closer to the lower-left image corner agree with positions of Fe xxiv and Ca xvii (lines of numbers 1 and 2 in table 1) lines which contributes to the signal in *TRACE* 195 Å channel at high temperatures. Position of the second, more extended structure closer

to the upper-right image corner agree with positions of the other lines listed in table 1 which live at much lower temperatures (see figure 10). The intensity maxima of these lines are at temperatures 1.6 MK - 3.2 MK.

Presence of a hot plasma in this flare is also seen in GOES data. A plot of GOES temperature time-line (obtained using filter ratio technique) for this event is shown in figure 11. At the time of the *TRACE* frame used for analysis (see figure 5) the GOES temperature determined in the isothermal approximation was 19 MK.

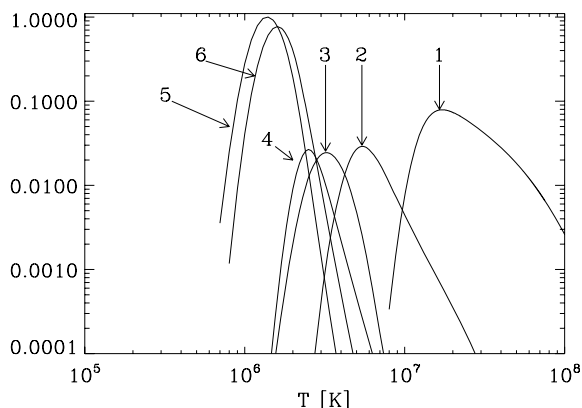


Figure 10. Principal coronal line emission curves for TRACE signal in 195 Å passband. Line numbers are the same as in table 1.

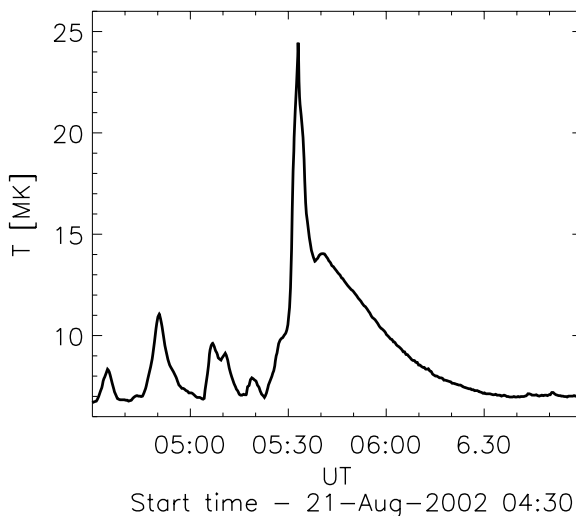


Figure 11. GOES temperature time-line for analyzed event.

## 4. CONCLUSIONS

We performed the analysis of the diffraction pattern seen in *TRACE* telescope EUV images. An image formation model was constructed in which the diffraction effects were included to *TRACE* PSF function.

It was found that the *TRACE* PSF shape strongly depends on temperature of the observed source particularly in far diffraction orders. This allows for application of spectroscopic methods to the *TRACE* data analysis.

We used the temperature variability of the *TRACE* PSF to determine T&EM distribution in the selected flare kernel. We found that in the twelfth diffraction order the kernel plasma separates into two components - hot plasma component ( $T > 10$  MK) and colder one. The positions of the hot component agree with position of emission contributed by Fe xxiv and Ca xvii principal lines for *TRACE* 195 channel. The colder component position agree with the position of emission that come from the others principal lines which has intensity maxima at temperatures 1.6 MK - 3.2 MK.

Presence of a hot plasma in this flare is also seen in GOES data. GOES temperature determined in the isothermal approximation was 19 MK for the time at which the selected for analysis *TRACE* frame was taken (2002-August-21 05:31:45).

We also found that using methods based on the *TRACE* PSF one can determine T&EM plasma distributions from single image (even if the emission site is saturated) for T up to 20 MK.

## ACKNOWLEDGMENTS

The authors would like to thank the SPM 11 meeting organizers for support.

## REFERENCES

- Gburek S., Sylwester J., Sylwester B., Kowalinski M.: 2004, *Proceedings of the 223 IAU symposium.*, 455.
- Handy, B., Acton, L., Kankelborg, C., et al. : 1999, *Solar Phys.*, **187**, 229.
- Phillips, K. J. H., Chifor, C., & Landi, E.: 2005, *ApJ.*, **626**, 1110.
- Lin, A., Nightingale, R, Tarbell, T. :2001, *Solar Phys.*, **198**, 385.
- Schrijver, C., Title, A., Berger, T., et al. :1999, *Solar Phys.*, **187**, 261.